Title

Integrated Structured Light Architectures: Review and Modeling

Author

He, Isabella

Publication Date

2024-10-01

Integrated Structured Light Architectures: Review and Modeling

Isabella He*[1]

[1]*UCLA, Materials Science and Engineering Department, 410 Westwood Plaza, Los Angeles, CA 90095*
**isabellahe@g.ucla.edu*

Abstract: A programmable light architecture is demonstrated using a hexagonal array of beams with individual amplitude, phase, polarization, and time tunability, exploiting more degrees of freedom of light to enable greater photonic device applications.

INTRODUCTION

Like structural color in nature, structured photonics can manipulate light and its field parameters and has implications in communications, quantum computing, and beyond. An existing approach to structured light manipulation uses spatial light modulators, which vary field polarization, magnitude, or phase with respect to space and time[1]. However, applications of spatial light modulators are limited due to their operational damage threshold and poor response to ultrashort pulses, meaning high power fields like free-space optical communications require an alternative approach, such as phased arrays. Arrays of coherent beams with phase control especially in vortex and orbital angular momentum (OAM) configurations have been successful in demonstrating circularly symmetric arrays with phase modulation. To implement phased arrays in a wider range of femtosecond pulse and power-scalable applications, these vortex and OAM beams may be adapted for additional control of other field defining parameters on top of phase and amplitude.

This study by Lemons et. al. focuses on a phased array architecture with individually programmable beams to produce complex intensity and phase profiles with real-time tuning. Building upon vortex and OAM beams, this architecture further allows control of carrier-envelope phase (CEP), pulse front, and polarization[2]. Numerical modeling and experimental results are investigated to validate the design and synthesis of the integrated architecture. Broadly, this proof of concept shows the potential to expand existing technology in light manipulation by exploiting more degrees of freedom to access greater quantum optics fields.

METHODS

To expand on OAM phased arrays, this study uses a new light architecture to take advantage of more attributes of light in an adaptable manner. Pictured in Figure 1, the proposed device uses 7 beamlines, or individually controlled beams, locked in phase relative to a central beamline based on CEP. CEP stabilization on the front end across all beamlines initializes consistent phase behavior. This phase relationship can be arbitrarily controlled, in addition to the phase, amplitude, polarization state, and timing using a field-programmable gate array (FPGA). The beamlines are carried by fibers and are subjected to phase modulation with piezoelectric fiber stretchers. Intensity, polarization, and timing are controlled by optic elements of a half waveplate, polarizing beam splitter, and quarter waveplates on a fiber pigtailed delay stage. The composite of the resulting beamlines is collimated while preserving polarization, then monitored by an avalanche photodiode. Phase modulation responds to the photodiode amplitude, converging beamline phase towards one (central) reference beamline.

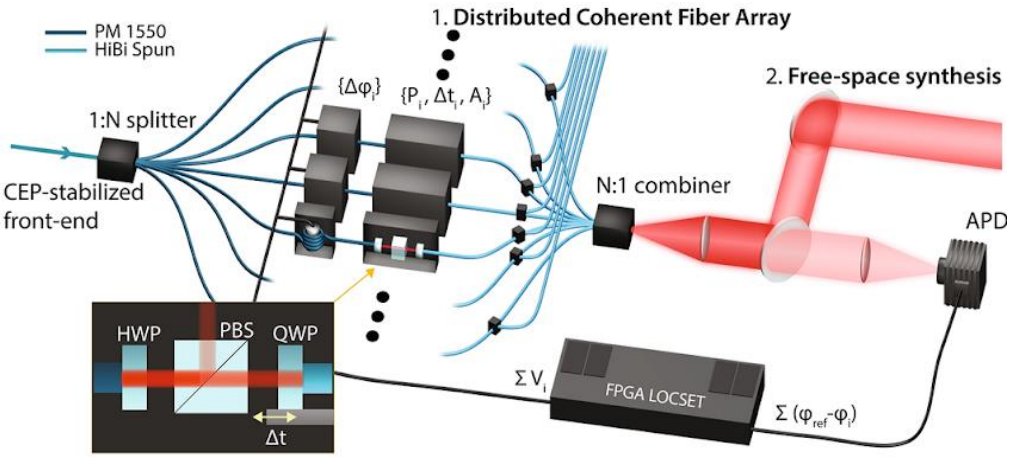

Fig. 1. The experimental configuration via coherent multi-channel coherent fiber array with a common CEP-stabilized front end, independent phase ($\Delta\varphi_i$), amplitude (A_i), polarization state ($\wp_i$), and timing (Δt_i) controls, and active locking via FPGA LOCSET using a single avalanche photodiode (APD) in the far-field. The output coherent output can be delivered in the form of a distributed coherent fiber array or the form of a free-space synthesized pulse. (Ref. [num], Fig. 1).

By only tuning amplitude and phase, this system of 7 beamlines demonstrates versatility in producing complex intensity and phase distributions. Relative amplitude of each beamline is described by A_k and phase is described by φ_k. Eight near-field phase and amplitude combinations are tested, their resulting far-field transverse intensity distribution and retrieved phase distributions are compared. Examples include a conventional coherent beam, cylindrically structured pulses, and cylindrically asymmetric pulses. Of particular interest is the case with total phase offset 2π increasing clock-wise monotonically and uniformly, which is analogous to a first-order (2π offset) and discretized OAM.

Numerical beam propagation is used to expand on the demonstrated 7+1 beam device and explore more advanced OAM beam replications by reducing discretization. A discrete fast Fourier transform angular spectrum method is used, assuming scalar propagation. To demonstrate the effect of discretization, modelling is performed for varied channel counts added in the hexagonal configuration. 7-channel, 19-channel, and 37-channel discretizations are compared to an ideal first-order OAM beam in intensity and phase distribution.

To illustrate the dynamic polarization topographies the experimental device can produce, topographic maps are derived from Stokes projections captured by a polarizing optical system with an InGaAs camera. Phase and amplitude values are maintained between beamlines and trials, varying only near-field polarization distribution to produce different topographic maps. Resulting polarization distributions are compared between alternating linear, asymmetric linear, and asymmetric circular polarization coherent synthesis near-field configurations.

RESULTS AND INTERPRETATION

The far-field intensity and phase profiles experimentally tested are similar to expected Laguerre-Gauss shapes for intensity and helical shapes for phase, but with some differences attributed to discretization. The range of phase distributions produced shows the flexibility of a 7+1 channel system, demonstrating great implications for more complex systems with more channels.

However, these results are not accompanied by the modeling parameters. The software cited[3][4] requires the definition of wavelength, real size, number of computational points, and initial

beam parameters. To investigate the replicability of the results, I kept the default parameters in a hexagonal tiling configuration, adjusting the waist size independently. I also varied propagation distance to visualize the far-field approximation in this model.

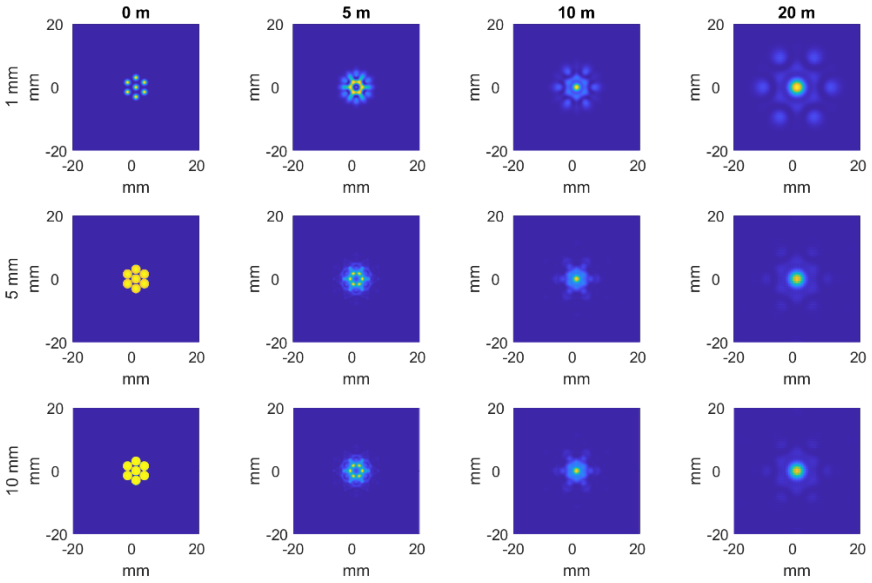

Fig. 2. Intensity distribution from varying input parameters. Each row is labeled with waist size (1, 5, 10 mm), and each column is labeled with propagation distance (initial, 5, 10, 20 m).

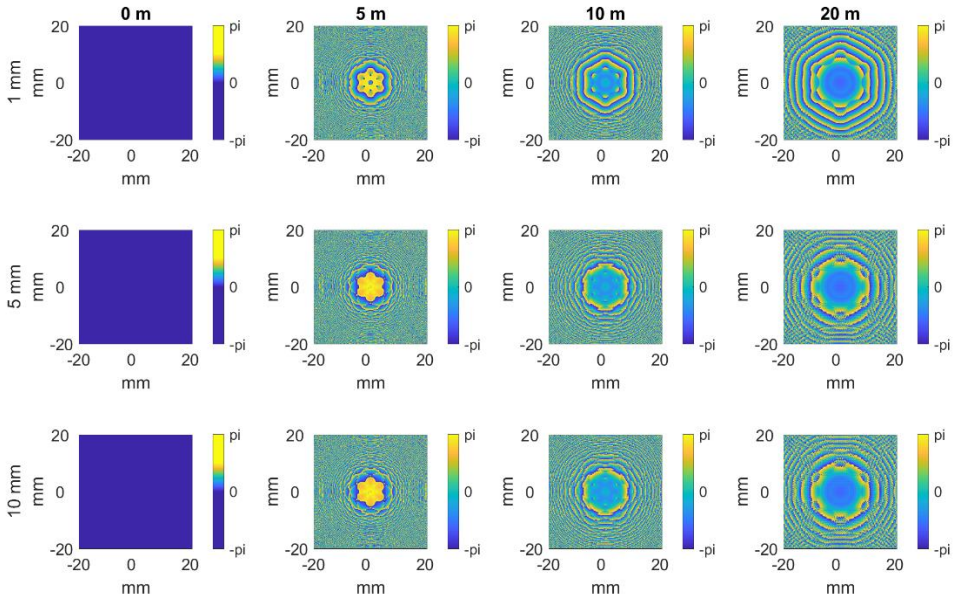

Fig. 3. Phase distribution from varying input parameters. Each row is labeled with waist size (1, 5, 10 mm), and each column is labeled with propagation distance (initial, 5, 10, 20 m).

Comparing intensity and phase distributions from Fig. 2 and Fig. 3, a 1 mm waist size and 20 m propagation most closely replicates the results of the original publication. Increasing waist size causes the intensity to decrease and reduces fidelity in the phase profile. This implies that waist size is an important factor in comparing these discrete channel configurations to ideal beams, as done in the following comparison to OAM beams.

Focusing on the OAM beam configuration, increasing channel count better approximates ideal behavior. To quantitatively characterize the effect of discretization, the mean squared error (MSE) in intensity was calculated between the ideal and 7-, 19-, and 37-channel configurations to be 0.0016, 0.001, and 0.0006, respectively.

Another significant result is the demonstration of programmable polarization topography, shown in Figure 3. Since these polarization distributions are controlled by three variables, $\Delta\varphi_i$, A_i, and $\wp_i$, even 7 channels allow a multitude of topographic maps. With greater channel number as suggested by optimization against discretization, the capacity to create programmable polarization topographies can be further enhanced and have real-world implications.

The last feature discussed is the optical delay control of the architecture (related to Δt_i of all beamlines), which is limited in range by the locking phase stability on the short end and the optical delay stages on the long stages. This capability thus expands on spatial light modulators in reaching short-pulse applications.

CONCLUSIONS

This study successfully demonstrates a new light architecture that uses amplitude, phase, polarization state, and timing of discrete beam sources to produce programmable coherent beam. The significance of this configuration compared to spatial light modulators and phased arrays are the implications of high power compatibility and greater spatio-temporal field control. For real-world applications, this general structure can be further investigated to optimize finesse in relation to complexity in increasing channel count. Ultimately, this architecture provides a potential solution to make greater optical applications previously not accessible by photonic devices.[5]

REFERENCES

1. Liu, J.-M. (2016). *Principles of photonics*. Cambridge university press.
2. Lemons, R., Liu, W., Frisch, J. C., Fry, A., Robinson, J., Smith, S. R., & Carbajo, S. (2021). Integrated structured light architectures. *Scientific Reports*, *11*(1), 796. https://doi.org/10.1038/s41598-020-80502-y
3. Lemons, R., & Carbajo, S. (2020). *Reconstruction and optimization of coherent synthesis by fourier optics based genetic algorithm* (arXiv:2005.13671). arXiv. https://doi.org/10.48550/arXiv.2005.13671
4. Lemons, R. & Carbajo, S. Coherent optics propagation and modeling. https://github.com/slaclab/CCPM/tree/1.0.0%0A.
5. Pelucchi, E., Fagas, G., Aharonovich, I., Englund, D., Figueroa, E., Gong, Q., Hannes, H., Liu, J., Lu, C.-Y., Matsuda, N., Pan, J.-W., Schreck, F., Sciarrino, F., Silberhorn, C., Wang, J., & Jöns, K. D. (2022). The potential and global outlook of integrated photonics for quantum technologies. *Nature Reviews Physics*, *4*(3), 194–208. https://doi.org/10.1038/s42254-021-00398-z